

## Adsorption of 1-(2-Thiazolylazo)-2-Naphthol on Amberlite XAD-7 and Silica Gel: Isotherms and Kinetic Studies

Grazielle C. Anaia,<sup>a</sup> Patricia A. M. Freitas,<sup>b</sup> Maria E. V. Suárez-Iha<sup>c</sup> and Fábio R. P. Rocha<sup>\*d</sup>

<sup>a</sup>Instituto de Química, Universidade de São Paulo, CP 26077, 05508-000 São Paulo-SP, Brazil

<sup>b</sup>Escola de Engenharia Mauá, Instituto Mauá de Tecnologia, 09580-900 São Caetano do Sul-SP, Brazil

<sup>c</sup>Escola de Engenharia, Universidade Presbiteriana Mackenzie, Rua da Consolação, 930, 01302-907 São Paulo-SP, Brazil

<sup>d</sup>Centro de Energia Nuclear na Agricultura, Universidade de São Paulo, CP 96, 13416-000 Piracicaba-SP, Brazil

O reagente 1-(2-tiazolilazo)-2-naftol (TAN) tem sido extensamente usado em extração em fase sólida (EFS) sem avaliação crítica do processo de adsorção. Neste trabalho, a adsorção de TAN em XAD-7 e sílica-gel foi investigada e os dados experimentais foram ajustados aos modelos de Langmuir, Freundlich e Dubinin-Radushkevich. Estes modelos forneceram bons ajustes para ambos adsorventes e seus respectivos parâmetros  $K_L$ ,  $K_F$  and  $K_{D,R}$  foram calculados. O tempo mínimo de contato de adsorção de TAN e a quantidade máxima de TAN adsorvido foram menores em XAD-7 (35 min e  $4,05 \times 10^{-3} \text{ g g}^{-1}$ ) em relação à sílica-gel (210 min e  $1,81 \times 10^{-2} \text{ g g}^{-1}$ ). A avaliação da energia de adsorção média caracterizou a adsorção como física e as superfícies para ambos os adsorventes como energeticamente heterogêneas. Os dados experimentais para ambos os sistemas mostraram excelentes ajustes ao modelo de pseudo-segunda ordem. Concordâncias entre  $q_{max,calc}$  e  $q_{max,exp}$  foram encontradas em todos os casos e a constante cinética confirmou o tempo mínimo diferente para alcançar adsorção máxima de TAN em XAD-7 e sílica-gel. Sílica gel pode ser apontada como o melhor adsorvente, considerando a capacidade de adsorção e a força de interação para adsorção de TAN.

The reagent 1-(2-thiazolylazo)-2-naphthol (TAN) has been extensively used in solid-phase extraction without a critical evaluation of the adsorption process. In this work, the adsorption of TAN onto XAD-7 and silica gel has been investigated and the experimental equilibrium data were fitted to the Langmuir, Freundlich and Dubinin-Radushkevich models. These models provided good fits for both adsorbents and their respective parameters  $K_L$ ,  $K_F$  and  $K_{D,R}$  were calculated. For the same TAN concentration range, the minimum time of contact for adsorption and the maximum amount of TAN adsorbed per gram were lower in XAD-7 (35 min and  $4.05 \times 10^{-3} \text{ g g}^{-1}$ ) than in silica gel (210 min and  $1.81 \times 10^{-2} \text{ g g}^{-1}$ ). The evaluation of the mean sorption energy characterized the adsorption as physical and the surfaces for both adsorbents as energetically heterogeneous. The experimental data for both systems showed an excellent adjustment to the pseudo-second order model. Excellent agreements between  $q_{max,calc}$  and  $q_{max,exp}$  were found in all cases and the kinetic constant value confirmed the different minimum time to reach maximum adsorption of TAN onto XAD-7 and silica gel. By considering the adsorption capacity and the force of the interaction, silica gel can be pointed out as the best support for adsorption of TAN.

**Keywords:** 1-(2-thiazolylazo)-2-naphthol, isotherms, adsorption, XAD-7 and silica gel

## Introduction

The reagent 1-(2-thiazolylazo)-2-naphthol (TAN) (Figure 1) is an orange solid produced by the diazotizing reaction of 2-aminothiazol with  $\text{NaNO}_2$  and subsequent reaction with 2-naphthol in alcoholic and alkaline medium.<sup>1</sup> In acid or strongly basic conditions, TAN is soluble due to the formation of positively ( $\text{HTAN}^+$ ) or negatively ( $\text{TAN}^-$ ) charged species, respectively, but in its neutral form, the reagent is only slightly soluble in water. This low solubility in water and their properties as chelating agent for transition metals make it suitable to adsorption procedures.<sup>2,3</sup>

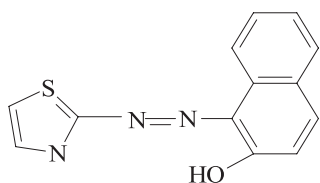


**Figure 1.** Chemical structure of the reagent 1-(2-thiazolylazo)-2-naphthol.

TAN is extensively used as chromogenic reagent for spectrophotometric determination of divalent metal ions, as well as in liquid-liquid extraction.<sup>4</sup> Several analytical applications have exploited solid-phase extraction,<sup>5,6</sup> including solid-phase spectrophotometry,<sup>7-10</sup> with TAN immobilized on  $\text{C}_{18}$  bonded silica. In spite of the good results attained, adsorption studies have not been carried out to select the best adsorbent aiming minimizing lixiviation of the immobilized reagent under the different acidity conditions used for retention and elution of the analytes.

Amberlite XAD are synthetic organic polymeric resins with excellent physical, chemical and thermal stability, large adsorption capacity, stability in a wide pH range and structural diversity. Their properties vary with surface area, polarity, particle size, porosity and percentage of cross linked bonds. The possibility to enhance the selectivity by modifying the surface with adsorbed organic reagents is attractive and several analytical applications have been reported in literature.<sup>11-14</sup> The Amberlite XAD-7 is a non ionic, ester acrylic polymer of aliphatic nature, macroporous structure and high surface area.<sup>15</sup> It has been used in solid phase extraction for determination of ultratrace levels and removal of metals in several samples,<sup>16-20</sup> equilibrium and adsorption studies<sup>21,22</sup> as well as in chromatographic separations.<sup>23,24</sup> Silica gel is an amorphous inorganic polymer of high mechanical resistance constituted by siloxane groups (Si-O-Si) in the internal part and by superficial silanol groups (Si-OH). Chemical and physical modifications are feasible by exploiting reactions with silanol groups in order to get novel materials suitable for analytical applications.<sup>25,26</sup>

The Langmuir model was originally proposed to describe the adsorption of gases on metallic surfaces. It represents sorption on a set of energetically equivalent adsorption sites, independent of the surface coverage and without interaction between adsorbed molecules.<sup>27</sup> The model allows evaluating the adsorption capacity, including the estimative of the equilibrium constant related to the adsorption process. Maximum adsorption is verified when surface of adsorbent is covered with a monolayer of adsorbate. The model allows applying experimental data in an extensive range of concentrations.<sup>28</sup> Equation 1 describes the Langmuir model in its non-linear form, which relates the adsorbed mass and the equilibrium concentration ( $C_{eq}$  / mol  $\text{L}^{-1}$ ).

$$q_{eq} = \frac{q_0 \times K_L \times C_{eq}}{1 + K_L \times C_{eq}} \quad (1)$$

where  $q_{eq}$  is the concentration of adsorbate at equilibrium ( $\text{g L}^{-1}$ );  $q_0$  is monolayer capacity of the maximum amount of solute adsorbed per gram of adsorbent ( $\text{g g}^{-1}$ ), i.e., the adsorption capacity and  $K_L$  is the Langmuir constant ( $\text{L g}^{-1}$ ) which is related to the adsorption equilibrium involving several factors, including physical, chemical and energetic characteristics. The linear equation 2 is obtained by rearrangement of equation 1:

$$\frac{1}{q_{eq}} = \frac{1}{q_0 \times K_L \times C_{eq}} + \frac{1}{q_0} \quad (2)$$

The Freundlich model<sup>29</sup> is useful to evaluate the energetic distribution of the adsorption sites on the surface characterized by the heterogeneity factor ( $n$ ). Adsorption can be defined as a process of molecules accumulation from a bulk solution onto the exterior and interior surfaces of an adsorbent and it may include various interactions such as hydrophobic, electrostatic attraction, and hydrogen bonding. Physical properties of the solid adsorbents like surface area, pore distribution, pore radius, and porosity, as well as chemical characteristics of the adsorbate, can also play an important role in the adsorption equilibria. The linear equation 3 expresses the quantitative relation between  $q_{eq}$  and  $C_{eq}$ .

$$\log q_{eq} = \log K_F + \frac{1}{n} \log C_{eq} \quad (3)$$

where  $K_F$  is an empirical constant which provides an indication of the adsorption capacity and  $1/n$  indicates the energetic heterogeneity of the adsorption sites;  $q_{eq}$  and  $C_{eq}$  have the same definitions as previously presented for Langmuir model.

The Dubinin-Radushkevich isotherm model<sup>30</sup> is based on the theory of the Polanyi potential sorption that assumes a fixed volume of sorption space close to the adsorbent and the existence of a sorption potential over these spaces. Equation 4 describes mathematically the model and equation 5 is used to calculate the energy involved on the adsorption process in order to distinguish between physical and chemical adsorption.

$$\ln q_{eq} = \ln K_{DR} - B \times \varepsilon^2 \quad (4)$$

$$E = \frac{1}{(-2 \times B)^{1/2}} \quad (5)$$

where  $q_{eq}$  is the amount of the adsorbate in the adsorbent at equilibrium ( $\text{mol L}^{-1} \text{g}^{-1}$ );  $K_{DR}$  is the Dubinin-Radushkevich constant related to the maximum amount adsorbed onto solid surface ( $\text{mol g}^{-1}$ );  $\varepsilon$  is the potential Polanyi  $\{\varepsilon = RT \ln[1+(1/C_{eq})]\}$ , in which  $R$  is the gas constant ( $8.314 \text{ J K}^{-1} \text{ mol}^{-1}$ ) and  $T$  is the temperature in Kelvin;  $E$  is the adsorption energy referring to the transfer of 1 mol of the adsorbate from the solution to the surface of the adsorbent ( $\text{kJ mol}^{-1}$ ) and  $B$  is related to the average sorption energy ( $E$ ).

Kinetic models are useful to investigate the adsorption mechanism. The differential equation 6 describes the pseudo-first order model,<sup>31</sup> where  $k_1$  ( $\text{min}^{-1}$ ) is the rate constant of pseudo-first order adsorption,  $q_{max}$  is the maximum amount of TAN adsorbed ( $q_{TAN}/q_{adsorbent}$ ) ( $\text{g g}^{-1}$ ) corresponding to the monolayer coverage and  $q_t$  is the amount of TAN on the surface of adsorbent ( $\text{g g}^{-1}$  adsorbent) when  $t \neq 0$ . Applying the boundary conditions,  $q_t = 0$  at  $t = 0$ , and the equilibrium condition,  $q_{ads} = q_t$  for each time  $t$ , equation 6 is converted in equation 7, whose linear regression supplies values of  $k_1$  and  $q_{max, calc}$ .

$$\frac{dq_t}{dt} = k_1(q_{max} - q_t) \quad (6)$$

$$\log(q_{max} - q_t) = \log q_{max, calc} - \frac{k_1}{2.303} t \quad (7)$$

The pseudo-second order model is mathematically described by equation 8,<sup>31</sup> where  $k_2$  ( $\text{g g}^{-1} \text{h}^{-1}$ ) is the rate constant of pseudo-second order adsorption,  $q_{max, calc}$  and  $q_t$  have the same meaning as in equation 7. Integrating equation 8 and applying the boundary condition  $q_t = 0$  at  $t = 0$ , and the equilibrium condition,  $q_{ads} = q_t$  for each time  $t$ , yield equation 9.

$$\frac{dq_t}{dt} = k_2(q_{max, calc} - q_t)^2 \quad (8)$$

$$\frac{t}{q_t} = \frac{1}{k_2 q_{max, calc}^2} + \frac{1}{q_{max, calc}} t \quad (9)$$

Adsorption involves diverse stages, where the rate-controlling step is the intraparticle diffusion mechanism. Close to the equilibrium, the intraparticle diffusion becomes slower due to the low concentration of adsorbate in solution. This possibility is dependent of the adsorbate amount and of the square root of time, as described by the Morris-Weber model,<sup>32</sup> expressed by the equation 10, where  $k_p$  is the intraparticle diffusion rate constant ( $\text{g g}^{-1} \text{min}^{-1/2}$ ). A plot of  $q_t \times t^{1/2}$  should then be a straight line with a slope corresponding to  $k_p$  when the intraparticle diffusion is a rate-limiting step and  $C$  is the intercept corresponding to the linear coefficient.

$$q_t = k_p t^{1/2} + C \quad (10)$$

In this work, kinetic and thermodynamic sorption studies of TAN on XAD-7 and silica gel were carried out aiming to select the best material for using in solid-phase extraction.

## Experimental

### Adsorbents, reagents and solutions

All reagents and solvents were of analytical grade. Stock solutions 0.1% (m/v) TAN were prepared in 72% ethanol (Merck) and 0.1% (m/v) Triton X-100 (Sigma) to increase TAN solubility. TAN working solutions were prepared by dilution of the stock with 0.1 mol L<sup>-1</sup> Triton X-100 and hexamine (Synth) buffer solution (0.1 mol L<sup>-1</sup>; pH = 6.5). These buffer and pH were selected by taking into account the use in previous works involving SPE.<sup>5-10</sup> As at pH 6.5 predominates the neutral form of TAN, the adsorption tend to be maximum.

Physicochemical properties of the adsorbents are shown in Table 1.<sup>15,33</sup> Silica gel (Aldrich), 60 Å, 230-400 mesh grade was used. Initially the material was washed with 0.1 mol L<sup>-1</sup> HCl solution for 24 h, for removing adsorbed metal ions and impurity traces. The solid was collected on a Büchner funnel with a filter paper and repeatedly washed with deionized water until the filtrate showed pH close to 6. The XAD-7 resin was thoroughly washed with 0.1 mol L<sup>-1</sup> HCl solution for 15 min to remove any impurities and the reagents NaCl and Na<sub>2</sub>CO<sub>3</sub> originally added to the resins in order to prevent the bacterial growth. The resin was filtered and washed in similar way. The washed silica and XAD-7 were dried in a desiccator for 4 days to remove adsorbed water.

**Table 1.** Physicochemical properties of silica gel and XAD-7 adsorbents<sup>15,33</sup>

Physicochemical property	Silica gel	XAD-7
Surface area / (m <sup>2</sup> g <sup>-1</sup> )	530	450
Particle size / mesh	230-400	20-40
Average pore volume / (cm <sup>3</sup> g <sup>-1</sup> )	0.80	1.14
Average pore diameter / Å	60	90
Total porosity / (cm <sup>3</sup> cm <sup>-3</sup> )	0.420	0.550
Dry/Wet density / (g cm <sup>-3</sup> )	1.07/1.02	1.24/1.05
Polarity	Polar	Polar (intermediate)

## Apparatus

The measurements were carried out with an UV-vis spectrophotometer (Femto, model 700 S) using 1.00-cm quartz cells (all adsorption experiments and the desorption studies in acid medium). A flow cell with 100-cm optical path (Ocean Optics), based on a Teflon® AF-2400 liquid-core waveguide was employed in the desorption studies from hexamine buffer.

The pH measurements were performed with a pH-meter (Metrohm 654) equipped with a glass electrode with the Ag/AgCl reference electrode filled with 3 mol L<sup>-1</sup> NaCl solution. The agitation of the mixtures was performed on a shaker (TE-140 Tecnal) with controlled velocity. An analytical balance (Sartorius BP 110S) and centrifuge (Spin IV, Incibras) were also used. The room temperature was kept in 25 ± 1 °C during all experiments.

The cuvettes and all vessels used in the experiments were washed with 10% (v/v) HNO<sub>3</sub> aqueous solution followed by distilled and deionized water to remove traces of contaminants.

## Adsorption and desorption studies

TAN adsorption kinetics was investigated using the solution depletion method. In polyethylene flasks with screw caps, 50.0 ± 0.1 mg of each resin was shaken for different periods (1 to 250 min) with 10.0 mL TAN solutions in hexamine buffer at pH 6.5. The sorbed amount of TAN at equilibrium was calculated by the difference (attenuation) in the absorbance of the aliquots drawn before and after shaking. TAN initial concentrations were fixed at 5.00 × 10<sup>-5</sup> and 9.02 × 10<sup>-5</sup> mol L<sup>-1</sup> for the systems XAD-7/TAN and silica gel/TAN, respectively. The supernatants were separated by centrifuging the mixtures and the remaining TAN concentration was determined by spectrophotometry at 488 nm, with a 1-cm optical path cell. The blank solutions were prepared in similar way but without TAN reagent.

For isotherm studies, glass flasks were preferred to minimize TAN adsorption at the tube walls. A mass of 1000.0 ± 0.1 mg of each material was shaken for 35 or 210 min, respectively, with 10.0 mL TAN aqueous solutions at pH 6.5. For the XAD-7/TAN and silica gel/TAN systems the TAN concentrations varied from 4.70 × 10<sup>-5</sup> to 1.10 × 10<sup>-4</sup> and from 6.30 × 10<sup>-5</sup> to 1.20 × 10<sup>-4</sup> mol L<sup>-1</sup>, respectively. The time of contact was based on the kinetic study and the experimental procedure was the same as described above.

Nitric acid solutions at 0.5 or 0.1 mol L<sup>-1</sup> and hexamine buffer 0.1 mol L<sup>-1</sup> solution (pH 6.5) were used to evaluate TAN desorption from the loaded adsorbents. In glass tubes, 1000.0 ± 0.1 mg of each adsorbent was shaken for 1 h with 10.0 mL of each solution. The supernatants were separated by centrifuging the mixtures and the concentration of TAN was determined by spectrophotometry at 441, 445 and 488 nm for 0.1 and 0.5 mol L<sup>-1</sup> HNO<sub>3</sub> and hexamine buffer solutions, respectively. The absorbance of the solutions in acidic and buffered media was measured in 1.00 and 100 cm optical path cells, respectively, due to the different amounts of TAN released.

## Results and discussion

### Adsorption isotherms

Due to its hydrophobic characteristics, TAN has been widely used for modification of solid materials aiming SPE of several metal ions. However, these hydrophobic characteristics make TAN only slightly soluble in water and addition of miscible organic solvents, surfactants or both are required for reagent dissolution. As the amount of these additives can affect the adsorption process, they were minimized and kept constant in all experiments, i.e., all solutions contained 0.1% (m/v) Triton X-100 and lower than 2% (v/v) ethanol.

TAN UV-vis spectra for aqueous solutions at pH 6.5 showed maximum absorption at 488 nm. The analytical curve for TAN at these pH and wavelength is described by equation 11 ( $r = 0.999$ ), in which  $A$  is the absorbance and  $C_{\text{TAN}}$  is the concentration of the azo-reagent in mol L<sup>-1</sup>. In aqueous solutions, TAN may have acid/base behaviors with two ionization constants ( $\text{p}K_1 = 2.36$  and  $\text{p}K_2 = 8.71$ ) therefore at pH 6.5 we can consider that the neutral species of TAN is predominant.

$$A_{488 \text{ nm}} = 1.36 \times 10^3 C_{\text{TAN}} + 0.0112 \quad (11)$$

Several experiments were conducted to assess the minimum time necessary to obtain a maximum adsorption of TAN onto XAD-7 resin and silica gel. These experiments

were carried out at pH 6.5 and  $5.00 \times 10^{-5} \text{ mol L}^{-1}$  TAN for XAD-7 and  $9.02 \times 10^{-5} \text{ mol L}^{-1}$  TAN for silica gel. The variation of the mass of TAN adsorbed per gram of adsorbent as a function of time is shown in Figure 2 for both materials. The maximum sorption of TAN was achieved after 35 min for XAD-7 (Figure 2a) and 210 min for silica gel (Figure 2b). The acrylic ester resin (XAD-7) then reaches equilibrium faster than silica gel. These minimum time intervals were fixed to obtain the adsorption isotherms and related parameters.

Experimental data in Figure 2 were obtained using only one TAN concentration aiming to determine the minimum interval necessary to reach the equilibrium. These times for TAN adsorption onto XAD-7 and silica gel were adopted for further experiments, when the initial concentration of TAN was varied. Then, the isotherm models were applied to determine the thermodynamic data by varying the adsorbate concentration with a fixed time for adsorption.

Adsorption studies are carried out in steady state condition in which the adsorbate in the solution bulk is involved in a dynamic equilibrium with the surface of the adsorbent. Knowledge of this process is required for better understanding features of the adsorbent/adsorbate system like their affinity or sorption capacity. Experimental values were obtained for the adsorption of TAN on silica gel and XAD-7 and three commonly used mathematical models were evaluated: Langmuir, Freundlich and Dubinin-Radushkevich.<sup>29,34</sup>

Figure 3 shows the experimental data  $1/q_{eq} \times 1/C_{eq}$  for XAD-7/TAN (a) and silica gel/TAN (b). The fit of these linear curves (minimum square method) resulted in correlation coefficients of 0.979 and 0.986, respectively, for XAD-7/TAN and silica gel/TAN. The parameters  $K_L$  are  $3.95 \times 10^5 \text{ L g}^{-1}$  and  $2.81 \times 10^2 \text{ L g}^{-1}$ , whereas  $q_0$  are  $4.05 \times 10^{-3} \text{ g g}^{-1}$  and  $1.81 \times 10^{-2} \text{ g g}^{-1}$  for XAD-7 and silica gel, respectively. The Langmuir parameters described in Table 2 indicate that the adsorption capacity for silica gel is

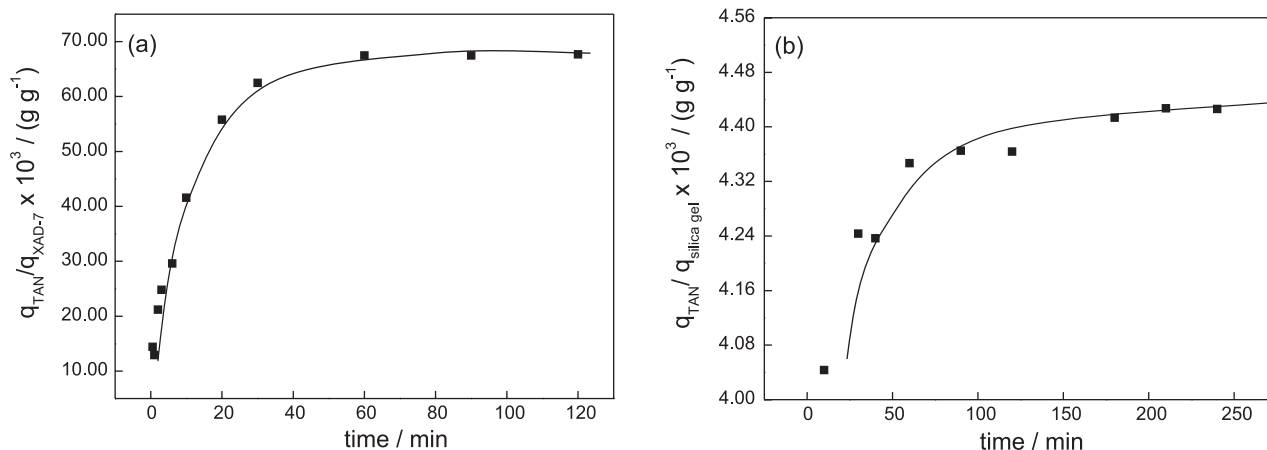


**Figure 2.** Effect of the contact time on the adsorbed mass of TAN *per* adsorbent mass at pH 6.5 (hexamine buffer): (a) XAD-7/TAN and (b) silica gel/TAN systems.

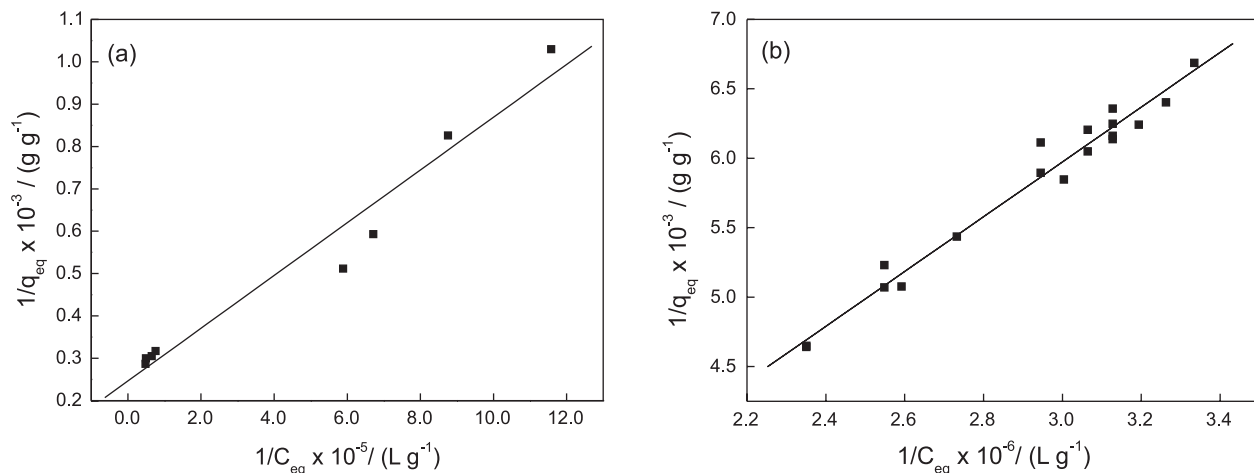


**Figure 3.** Adsorption isotherms (Langmuir model) of TAN onto (a) XAD-7 and (b) silica gel at pH 6.5 and  $25 \pm 1 \text{ }^\circ\text{C}$ .

4.5-fold higher than on XAD-7. This may be correlated with the higher surface area and lower pore size for silica gel (Table 1) which present important effects on the adsorption capacity. The  $K_L$  constants indicate higher bonding energy of TAN on XAD-7 than on silica gel.

The Freundlich parameters  $1/n$  and  $K_F$  were calculated from the slope and intercept of the plots  $\log q_{eq} \times \log C_{eq}$  (Figure 4). The high correlation coefficients ( $r = 0.993$  and  $0.998$  for XAD-7 and silica gel, respectively) show that the model is very suitable for describing the adsorption systems in the studied concentration ranges, thus yielding  $K_F$  and  $n$  values showed on Table 2. The Freundlich adsorption isotherm does not predict any saturation of the solid adsorbent surface, therefore the infinite coverage is predicted mathematically. Adsorption on silica gel shows a  $K_F$  value ( $2.27 \text{ g g}^{-1}$ ) 10-fold higher than the corresponding XAD-7 value ( $K_F = 0.232 \text{ g g}^{-1}$ ) which represents a stronger interaction between TAN and the silica gel than that with XAD-7. The values of  $n$  obtained for the adsorption of

TAN in both adsorbents were higher than 1, indicating favored adsorption and that the process for both adsorbents is energetically heterogeneous.

In order to distinguish between physical and chemical adsorption, the experimental data were applied to a Dubinin-Radushkevich isotherm model.<sup>34</sup> A linear plot of  $\ln q_{eq} \times \epsilon^2$  (Figure 5) yielded linear correlation coefficients of 0.992 and 0.808 for XAD-7/TAN and silica gel/TAN, respectively. The calculated values (Table 2) of  $B$  and  $K_{DR}$  from the slope and the intercept are  $(-2.65 \times 10^{-9} \text{ J}^2 \text{ mol}^{-2})$  and  $0.196 \text{ mol g}^{-1}$  for XAD-7/TAN and  $(-1.15 \times 10^{-6} \text{ J}^2 \text{ mol}^{-2})$  and  $27.5 \text{ mol g}^{-1}$  for silica gel/TAN. The numerical values of  $E$  calculated from equation 6 are  $13.7 \text{ kJ mol}^{-1}$  for XAD-7/TAN and  $7.07 \text{ kJ mol}^{-1}$  for silica gel/TAN. As these energy values are lower than  $42 \text{ kJ mol}^{-1}$ , the adsorption of TAN on both adsorbents can be considered as physical.<sup>35</sup> Weak physical intermolecular forces acting on adsorbent surface are attributed to van der Waals or hydrogen bonding.<sup>36</sup>

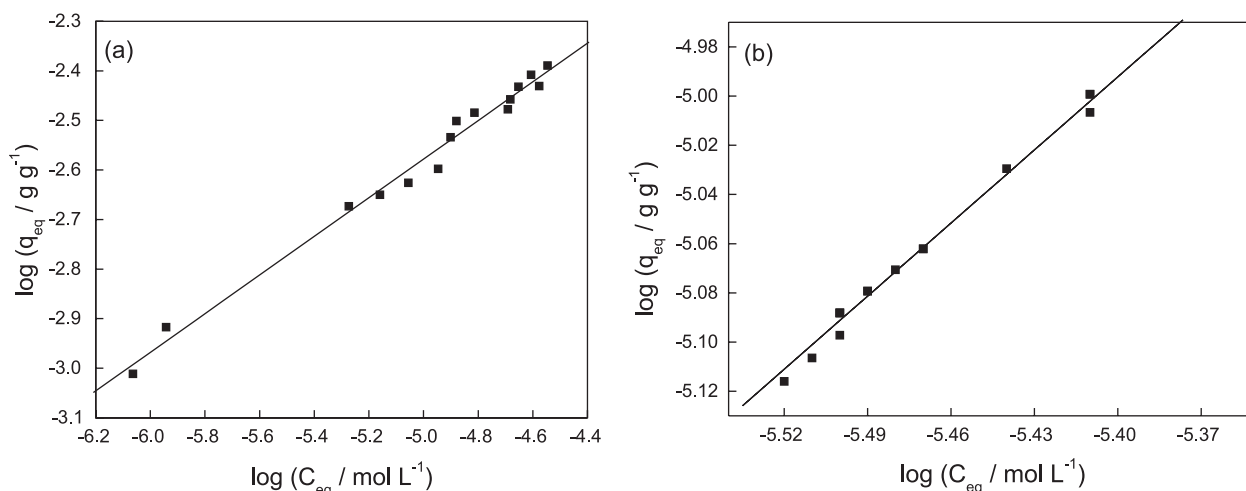


**Figure 4.** Adsorption isotherms (Freundlich model) of TAN onto (a) XAD-7 and (b) silica gel at pH = 6.5 and  $25 \pm 1$  °C.

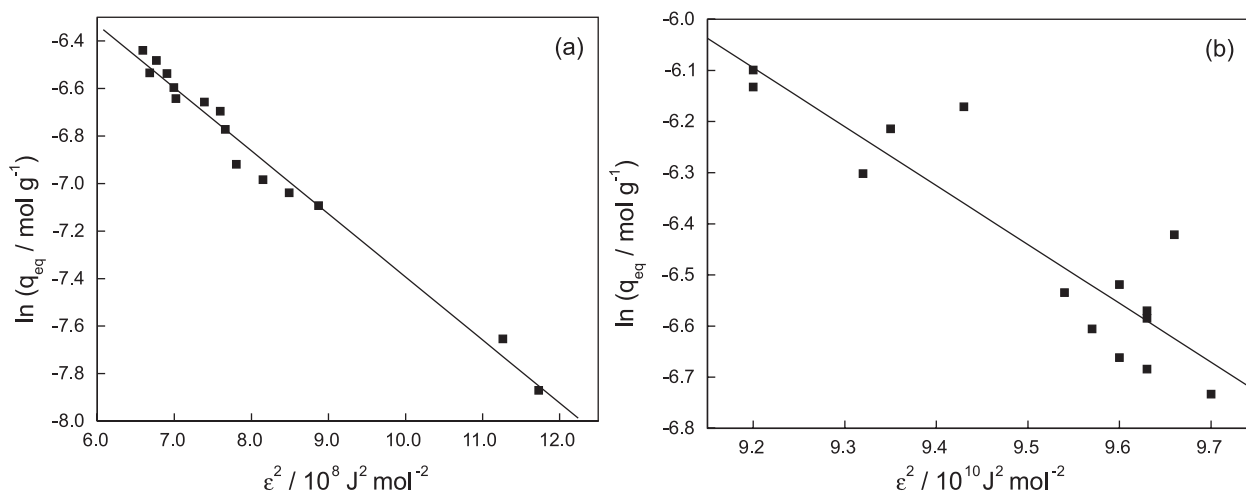


**Figure 5.** Adsorption isotherms of TAN (Dubinin-Radushkevich model) onto (a) XAD-7 and (b) silica gel at pH = 6.5 and  $25 \pm 1$  °C.



**Table 2.** Parameters of Langmuir, Freundlich and Dubinin-Radushkevich models for adsorption of TAN on silica gel and XAD-7. Symbols are defined in the text

Adsorbent	Langmuir		Freundlich		Dubinin-Radushkevich		
	$K_L / (\text{L g}^{-1})$	$q_0 / (\text{g g}^{-1})$	$K_F / (\text{g g}^{-1})$	$n$	$K_{DR} / (\text{mol g}^{-1})$	$B / (\text{J}^2 \text{mol}^{-2})$	$E / (\text{kJ mol}^{-1})$
silica gel	$2.81 \times 10^2$	$1.81 \times 10^{-2}$	2.27	1.01	27.5	$-1.15 \times 10^{-6}$	7.07
XAD-7	$3.95 \times 10^5$	$4.05 \times 10^{-3}$	0.232	2.57	0.196	$-2.65 \times 10^{-9}$	13.7

Freitas *et al.*<sup>37</sup> applied the Langmuir, Freundlich and Dubinin-Radushkevich models to evaluate the adsorption of monoethanolamine (MEA) and di-2-pyridyl ketone salicyloylhydrazone (DPKSH) on XAD-7. The results obtained with these systems are shown in Table 3 for comparison with those attained with TAN under similar conditions. According to the Langmuir model, XAD-7/TAN system shows the highest  $K_L$  constant. This feature is own of each system and reflects chemical, physical and energetic factors. The formation of a monolayer at equilibrium, evaluated by maximum mass of adsorbate per gram of the adsorbent is lower for XAD-7/TAN than for XAD-7/MEA. The XAD-7/DPKSH system showed the highest  $q_0$  value among the three systems indicating that a high quantity of DPKSH composes the monolayer in the surface of the adsorbent. For all systems,  $n$  was higher than 1, indicating the energetic heterogeneity of the adsorption sites, which corroborates the results obtained in the present study with the same adsorbent. The force of contact, evaluated by the Freundlich constant ( $K_F$ ), was higher for XAD-7/MEA than for XAD-7/TAN, showing that MEA seems to be more strongly adsorbed in XAD-7. For XAD-7/DPKSH, the parameter  $K_F$  was the lowest, probably due to the high esteric hindrance of the adsorbate, which contains three aromatic rings. For all systems, the adsorption energy ( $E / \text{kJ mol}^{-1}$ ) referring to the transference of 1 mol of adsorbate (TAN, MEA or DPKSH) from the solution to the surface of the adsorbent was lower than  $42 \text{ kJ mol}^{-1}$ , thus indicating a physical adsorption, which involves weak binding energies (van der Waals energy).<sup>29</sup>

#### Adsorption kinetics

Aiming to investigate the adsorption mechanism for the XAD-7/TAN and silica gel/TAN systems, pseudo-first

order (Langergren), pseudo-second-order and intraparticle diffusion models were applied to the experimental data. Spectra of the supernatant solutions were obtained after the contact with the adsorbents in different TAN concentrations and time periods. Figure 6 presents the experimental curves of the variation of the TAN mass adsorbed in function of time for different initial concentrations of TAN for XAD-7 (Figure 6A) and silica gel (Figure 6B).

By applying the pseudo-first order model, linear correlation was not found to the experimental data for silica gel adsorbent. Such behavior was observed in the whole contact time and initial concentrations evaluated. This poor correlation indicates that TAN does not adsorb onto material occupying only one adsorption site.

For XAD-7/TAN, a good linear correlation between  $\log(q_{max} - q_t)$  and  $t$  ( $r > 0.996$ ), was observed only at low TAN concentrations and the first 10 min, thus indicating that this system follows the pseudo-first order mechanism. In comparison to the silica gel-TAN system, higher values of pseudo-first order constants ( $k_i$ ) were found:  $0.475$  and  $0.359 \text{ g g}^{-1} \text{ min}^{-1}$  for initial TAN concentrations of  $2.00$  and  $4.00 \times 10^{-5} \text{ mol L}^{-1}$ , respectively. These higher rates are associated to a large number of sites that are available for adsorption. For higher initial TAN concentrations a different behavior was observed, in general the rates were lower and with some tendency to be constant with the increase of TAN concentration. This behavior can be explained by considering that part of the adsorbate molecules occupy two adsorption sites on the solid surface instead only one, showing an interesting double behavior.

The adsorption kinetics may also be described by a pseudo-second order model (equations 8 and 9). Experimental data of  $t/q_t$  were registered as function of time for both systems and good linear correlation coefficients ( $r > 0.996$ ) were found for all adsorbate/adsorbent contact

**Table 3.** Parameters of Langmuir, Freundlich and Dubinin-Radushkevich isotherms for adsorption of TAN, MEA and DPKSH<sup>37</sup> on XAD-7

	Langmuir		Freundlich		Dubinin-Radushkevich	
	$K_L / (\text{L g}^{-1})$	$q_0 / (\text{g g}^{-1})$	$K_F / (\text{g g}^{-1})$	$N$	$K_{DR} / (\text{mol g}^{-1})$	$E / (\text{kJ mol}^{-1})$
TAN	$3.95 \times 10^5$	$4.05 \times 10^{-3}$	0.232	2.57	0.196	13.7
MEA	$3.06 \times 10^4$	$5.18 \times 10^{-3}$	4.41	1.40	0.0840	9.78
DPKSH	$1.17 \times 10^2$	$1.04 \times 10^{-2}$	0.170	1.30	0.0663	9.54

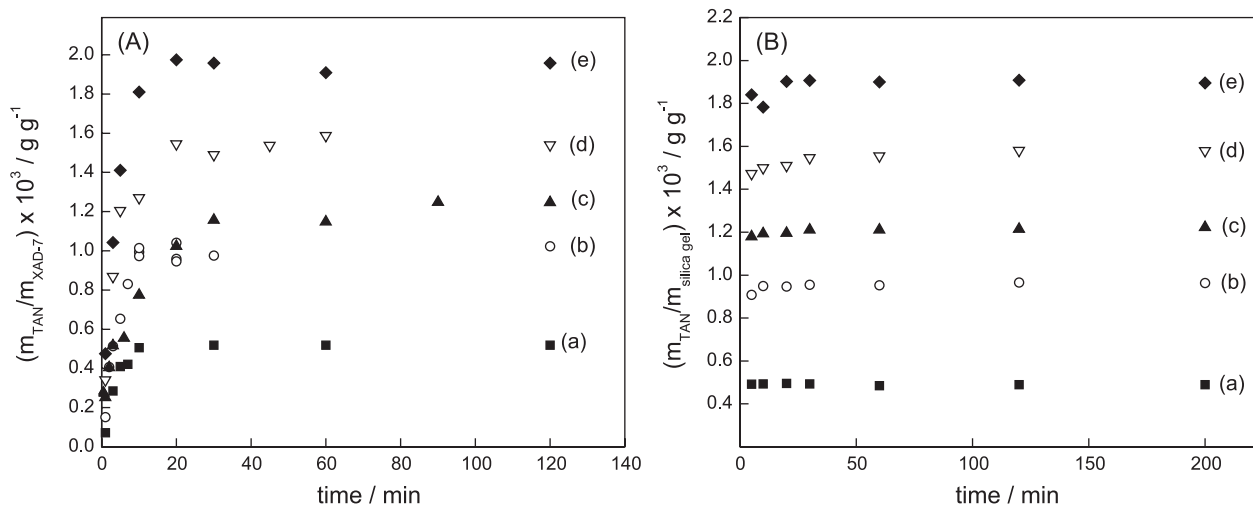


**Figure 6.** Dependence of adsorbed mass of TAN per gram of the adsorbents on time of contact: (A) XAD-7 and (B) silica gel. TAN initial concentrations: (a)  $2.00 \times 10^{-5}$ , (b)  $4.00 \times 10^{-5}$ , (c)  $5.02 \times 10^{-5}$ , (d)  $6.47 \times 10^{-5}$  and (e)  $8.00 \times 10^{-5}$  mol L<sup>-1</sup>; pH = 6.5.

times and initial TAN concentrations investigated. This agreement shows that the adsorption follows a pseudo-second order mechanism and that adsorbate bonds to two active adsorption sites on both silica gel and XAD-7 surface. Values of  $q_{max,calc}$  and  $k_2$  calculated for both systems are shown in Table 4.

For both materials, in the lowest initial concentration ( $2.00 \times 10^{-5}$  mol L<sup>-1</sup>), the large number of adsorption sites favored the adsorption and consequently,  $k_2$  presents a higher value for silica gel ( $6.35 \times 10^{-2}$  min<sup>-1</sup>) than for XAD-7 ( $0.802 \times 10^{-2}$  min<sup>-1</sup>). However, considering all TAN initial concentrations, values of  $k_2$  show an irregular variation. A minimum value was observed and then,  $k_2$  tends to a constant value, independent of the initial concentration. Although a pseudo-first order behavior had been observed for XAD-7/TAN it was showed only for low contact time (10 min). Therefore, by considering

the whole time interval and TAN concentrations, we can assume that the both systems follow the pseudo-second order model.

The intraparticle diffusion model was applied to experimental data obtained in different initial concentrations (Figure 7). Non-linear plots were observed over the whole range of time (multilinearity) indicating that other processes drive the adsorption of TAN on XAD-7. In general, a first sharper portion of the curve may be considered as an external surface adsorption or a faster adsorption stage. A second portion is a gradual adsorption stage, where intraparticle diffusion is rate-controlled. The third portion is attributed to the final equilibrium stage where the intraparticle diffusion is slower due to the extremely low adsorbate concentrations in solution. The rate of uptake might be limited by size of adsorbate molecule, concentration of the adsorbate and its affinity to the adsorbent, diffusion coefficient of the

**Table 4.** Results of pseudo-second order adsorption model for TAN on XAD-7 and silica gel at pH 6.5

XAD-7/TAN				
$C_{TAN} / (10^{-5} \text{ mol L}^{-1})$	$k_2 / (10^2 \text{ min}^{-1})$	$q_{ads,calc}^{max} / (10^{-3} \text{ g g}^{-1})$	$q_{ads,exp}^{max} / (10^{-3} \text{ g g}^{-1})$	r
2.00	6.35	0.596	0.518	0.998
4.00	4.48	1.05	1.01	0.999
5.02	1.56	1.29	1.25	0.999
6.47	3.36	1.59	1.56	0.999
8.00	3.06	1.98	1.96	0.999
SILICA GEL/TAN				
2.00	0.802	0.493	0.494	0.999
4.00	0.297	0.963	0.965	0.999
5.02	0.211	1.22	1.21	0.999
6.47	0.0881	1.59	1.58	0.999
8.00	0.524	1.90	1.90	0.999



adsorbate in the bulk phase, the pore-size distribution of the adsorbent and degree of mixing.

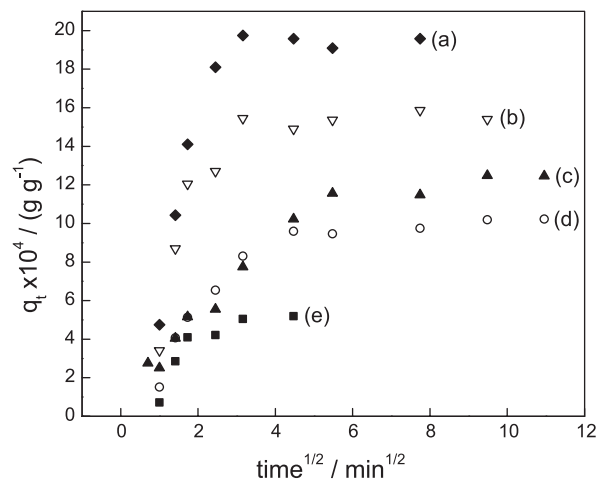


**Figure 7.** Intraparticle diffusion model for XAD-7/TAN system for initial concentrations of: (a)  $2.00 \times 10^{-5}$ , (b)  $4.00 \times 10^{-5}$ , (c)  $5.02 \times 10^{-5}$ , (d)  $6.47 \times 10^{-5}$  and (e)  $8.00 \times 10^{-5}$  mol L<sup>-1</sup>.

Values of  $k_p$  ( $\text{g g}^{-1} \text{min}^{-1/2}$ ) and the correlation coefficients for all TAN initial concentrations investigated are in Table 5. High correlation coefficient ( $r > 0.97$ ) is found to the range of the experimental data to the diffusion model. The second portion of the curves can be attributed to intraparticle diffusion and an irregular variation of the diffusion rate with the initial TAN concentration was observed. An irregularity of the  $k_p$  values was also reported by Al-Ghout *et al.*<sup>38</sup> that can be related to either the heterogeneity of the material or the capability of adsorbate molecules to agglomerate on its surface. Deviations from the model were not observed in the highest initial concentration of TAN ( $8.00 \times 10^{-5}$  mol L<sup>-1</sup>), whereas this behavior may be observed if some repulsion

**Table 5.** Intraparticle diffusion adsorption model parameters of TAN on XAD-7 in various initial concentrations

$C_0 /$ ( $10^{-5}$ mol L <sup>-1</sup> )	$k_p /$ ( $10^{-4}$ g g <sup>-1</sup> min <sup>-1/2</sup> )	$C /$ ( $10^{-4}$ g g <sup>-1</sup> )	$r$
2.00	2.75	-1.99	0.999
4.00	3.73	-1.67	0.996
5.02	1.33	0.208	0.985
6.47	7.01	-3.55	0.999
8.00	6.17	-7.08	0.994

**Table 6.** Results of desorption studies of the adsorbents modified with TAN

Solution	XAD-7 ( $q_{\text{TAN des}}/q_{\text{TAN ads}} / (\text{g g}^{-1})$ )	Desorption / %	Silica gel ( $q_{\text{TAN des}}/q_{\text{TAN ads}} / (\text{g g}^{-1})$ )	Desorption / %
0.1 mol L <sup>-1</sup> HNO <sub>3</sub>	$3.83 \times 10^{-6}$	0.0946	$3.88 \times 10^{-4}$	2.14
0.5 mol L <sup>-1</sup> HNO <sub>3</sub>	$5.21 \times 10^{-5}$	1.29	$5.11 \times 10^{-4}$	2.82
0.1 mol L <sup>-1</sup> hexamine, pH 6.5	$2.17 \times 10^{-5}$	0.536	$1.26 \times 10^{-5}$	0.0696

adsorbent/adsorbate or adsorbate/adsorbate happens.<sup>39</sup> Intercept values of the linear diffusion segments does not pass through the origin of the graphic plot indicating that intraparticle diffusion is not the single rate-controlling mechanism. For silica gel/TAN system, it was not possible to observe any linear portion in the plot of  $q_t \times t$  for all TAN initial concentrations ( $2.00 \times 10^{-5}$  to  $8.00 \times 10^{-5}$  mol L<sup>-1</sup>), then  $k_p$  values were not calculated.

#### Desorption of TAN from the modified materials

Desorption studies of TAN were accomplished for both adsorbents modified with the azo-reagent for HNO<sub>3</sub> (0.1 and 0.5 mol L<sup>-1</sup>) and 0.1 mol L<sup>-1</sup> hexamine buffer, employing 1 h of contact time. These solutions were selected by considering applications of TAN immobilized on solid supports for separation and concentration of metal ions,<sup>5-10</sup> in which a buffered medium (e.g., hexamine buffer) is used in the loading step and a diluted solution of a strong acid (e.g., HNO<sub>3</sub>) is used for elution. In the elution step, undesirable desorption of TAN (weakly bounded to XAD-7 and silica gel by van der Waals forces) can occur due to the formation of the protonated species (HTAN<sup>+</sup>). The analytical wavelengths for aqueous solutions in acid medium and hexamine buffer were established at 445 and 488 nm, respectively.

According to the results shown in Table 6, the highest leaching was observed for 0.5 mol L<sup>-1</sup> HNO<sub>3</sub> followed by 0.1 mol L<sup>-1</sup> HNO<sub>3</sub> and hexamine buffer. These differences are associated to the acid-base equilibria involved. TAN is more soluble in acidic solution due to the formation of positively charged species (HTAN<sup>+</sup>). In hexamine buffer solution at pH 6.5 predominates the neutral form and then the mass of TAN desorbed is reduced. Desorption percent was estimated by considering initial concentration  $q_0$  as  $4.05 \times 10^{-3}$  g g<sup>-1</sup> and  $1.81 \times 10^{-2}$  g g<sup>-1</sup> for XAD-7 and silica gel, respectively.

#### Conclusions

The adsorption capacity of TAN was suitably described by Langmuir, Freundlich and Dubinin-Radushkevich models and it was found to be higher onto silica gel than XAD-7. According to Langmuir model, silica gel presents a mass

of TAN adsorbed ( $1.81 \times 10^{-2} \text{ g g}^{-1}$ ) about 4.5 times higher than XAD-7 ( $4.05 \times 10^{-3} \text{ g g}^{-1}$ ). In addition, according to Freundlich model, a higher  $K_F$  value was obtained for silica gel (2.27) in comparison to XAD-7 (0.232) indicating a stronger adsorption capacity for silica gel and the  $n$  values correspond to an energetically heterogeneous surface. The pseudo-second order kinetic model best describes the sorption kinetic for both systems, thus suggesting that the interaction of each molecule of TAN occurs by the occupation of two sites on the surface of both adsorbents. In spite of lower desorption of TAN adsorbed in XAD-7 in acid media, by considering the adsorption capacity and the force of the interaction TAN/adsorbent, silica gel can be pointed as the best support for adsorption of TAN.

## Acknowledgements

The authors acknowledge the fellowships and financial support from the Brazilian agencies CNPq, CAPES and FAPESP.

## References

- Omar, M. M.; Mohamed, G. G.; *Spectrochim. Acta* **2005**, *61*, 929.
- Ueno, K.; Imamera, T.; Cheng, K. L.; *Handbook of Organics Analytical Reagents*, 1<sup>st</sup> ed., CRC Press Florida, 1982.
- Lee, W.; Lee, S. E.; Lee, C. H.; Kim, Y. S.; *Microchem. J.* **2001**, *70*, 195.
- Xue, A. F.; Qian, S. H.; He, G. Q. H.; Han, X. F.; *Analyst* **2001**, *126*, 239.
- Zaporozhets, O.; Petruniok, N.; Bessarabova, O.; Sukhan, V.; *Talanta* **1999**, *49*, 899.
- Hosseini-Bandegharai, A.; Hosseini, M. S.; Jalalabadi, Y.; Sarwghadia, M.; Nedaie, M.; Taherian, A.; Ghaznavi, A.; Eftekhari, A.; *Chem. Eng. J.* **2011**, *168*, 1163.
- Teixeira, L. S. G.; Rocha, F. R. P.; Korn, M.; Reis, B. F.; Ferreira, S. L. C.; Costa, A. C. S.; *Anal. Chim. Acta*, **1999**, *383*, 309.
- Teixeira, L. S. G.; Rocha, F. R. P.; Korn, M.; Reis, B. F.; Ferreira, S. L. C.; Costa, A. C. S.; *Talanta* **2000**, *51*, 1027.
- Teixeira, L. S. G.; Costa, A. C. S.; Garrigues, S.; de la Guardia, M.; *J. Braz. Chem. Soc.* **2002**, *13*, 54.
- Teixeira, L. S. G.; Rocha, F. R. P.; *Talanta* **2007**, *71*, 1507.
- Saberyan, K.; Zolfonoun, E.; Shamsipur, M.; Salavati-Niasari, M.; *Sep. Sci. Technol.* **2009**, *44*, 1851.
- Jain, V. K.; Mandalia, H. C.; Gupte, H. S.; Vyas, D. J.; *Talanta* **2009**, *79*, 1331.
- Kara, D.; Fischer, A.; Hill, S. J.; *J. Hazard. Mater.* **2009**, *165*, 1165.
- Sharma, R. K.; Pant, P.; *Int. J. Environ. Anal. Chem.* **2009**, *89*, 503.
- Technical Information Bulletin Amberlite XAD-7 Industrial Grade Polymeric Adsorbent*; Rohm & Haas Co.: Philadelphia, 2003.
- Divrikli, U.; Akdogan, A.; Soylak, M.; Elci, L.; *J. Hazard. Mater.* **2007**, *149*, 331.
- Gallard, V.; Navarro, R.; Saucedo, L.; Avila, M.; Guibal, E.; *Sep. Sci. Technol.* **2008**, *44*, 2434.
- Yaman, M.; Ince, M.; *At. Spectrosc.* **2006**, *27*, 186.
- Matsumiya, H.; Yasuno, S.; Iki, N.; Myiano, S.; *J. Chromatogr., A* **2005**, *1090*, 197.
- Korn, M. G. A.; Santos Jr, A. F.; Jaeger, H. V.; Silva, N. M. S.; Costa, A. C. S.; *J. Braz. Chem. Soc.* **2004**, *15*, 212.
- Zhang, W.; Xu, Z.; Pan, B.; Hong, C.; Jia, K.; Jiang, P.; Zhang, Q.; *J. Colloid Interface Sci.* **2008**, *325*, 41.
- Balagi, T.; Matsunaga, H.; *Anal. Sci.* **2002**, *18*, 1345.
- Douse, J. M. F.; *J. Chromatogr. A* **1985**, *328*, 155.
- Macrae, T. G.; Gregson, R. P.; Quinn, R. J.; *J. Chromatogr. Sci.* **1982**, *20*, 475.
- Prado, A. G. S.; Faria, E. A.; Padilha, P. M.; *Quim. Nova* **2005**, *28*, 544.
- Lazarin, A. M.; Borgo, C. A.; Gushikem, Y.; *Quim. Nova* **2002**, *25*, 499.
- Sari, A.; Mendil, D.; Tuzen, M.; Soylak, M.; *J. Hazard. Mater.* **2009**, *162*, 874.
- Peric, J.; Trgo, M.; Medvidovic, N. V.; *Water Res.* **2004**, *38*, 1893.
- Foo, K. Y.; Hameed, B. H.; *Chem. Eng. J.* **2010**, *156*, 2.
- Dabrowski, A.; *Adv. Colloid and Interface Sci.* **2001**, *93*, 135.
- Cheung, W. H.; Mickay, G. J.; *Chem. Technol. Biotechnol.* **2003**, *78*, 562.
- Wu, F. -C.; Tseng, R. -L.; Juang, R. -S.; *Chem. Eng. J.* **2009**, *153*, 1.
- Data sheet product Silica Gel. <http://www.sigmaaldrich.com/catalog/product/fluka>, accessed in October 2013.
- Do, D. D.; *Adsorption Analysis: Equilibria and Kinetics*, 1<sup>st</sup> ed.; Imperial College Press: London, 1998.
- Zhang, W.; Xu, Z.; Pan, B.; Hong, C.; Jia, K.; Jiang, P.; Zhang, Q.; *J. Colloid Interface Sci.* **2008**, *325*, 41.
- Bakouri, H. E.; Usero, J.; Morillo, J.; Ouassini, A.; *Bioresour. Technol.* **2009**, *100*, 4147.
- Freitas, P. A. M.; Iha, K.; Felinto, M. C. F. C.; Suárez-Iha, M. E. V.; *J. Colloid Interface Sci.* **2008**, *323*, 1.
- Al-Ghout, M. A.; Khraisheh, M. A. M.; Ahmad, M. N. M.; Allen, S.; *J. Hazard. Mater.* **2009**, *165*, 589.
- Crini, G.; Peindy, H. N.; Gimbert, F.; Robert, C.; *Sep. Purif. Technol.* **2007**, *53*, 97.

Submitted on: July 02, 2013

Published online: January 21, 2014